applied sciences

MDPI

Article

Reduction of Liquid Bridge Force for 3D Microstructure Measurements

Hiroshi Murakami [1,*], Akio Katsuki [2], Takao Sajima [2] and Mitsuyoshi Fukuda [1]

[1] Department of Mechanical Systems Engineering, Faculty of Environmental Engineering, The University of Kitakyushu, 1-1 Hibikino, Wakamatsu-ku, Kitakyushu, Fukuoka 808-0135, Japan; v4mba020@eng.kitakyu-u.ac.jp

[2] Department of Mechanical Engineering, Faculty of Engineering, Kyushu University 744, Motooka, Nishi-ku, Fukuoka 819-0395, Japan; kaetrsuki@gmail.com (A.K.); sajima@mech.kyushu-u.ac.jp (T.S.)

* Correspondence: murakami@kitakyu-u.ac.jp; Tel.: +81-93-695-3201

Academic Editor: Kuang-Cha Fan

Received: 14 April 2016; Accepted: 11 May 2016; Published: 16 May 2016

Abstract: Recent years have witnessed an increased demand for a method for precise measurement of the microstructures of mechanical microparts, microelectromechanical systems, micromolds, optical devices, microholes, *etc.* This paper presents a measurement system for three-dimensional (3D) microstructures that use an optical fiber probe. This probe consists of a stylus shaft with a diameter of 2.5 μm and a glass ball with a diameter of 5 μm attached to the stylus tip. In this study, the measurement system, placed in a vacuum vessel, is constructed suitably to prevent adhesion of the stylus tip to the measured surface caused by the surface force resulting from the van der Waals force, electrostatic force, and liquid bridge force. First, these surface forces are analyzed with the aim of investigating the causes of adhesion. Subsequently, the effects of pressure inside the vacuum vessel on surface forces are evaluated. As a result, it is found that the surface force is 0.13 μN when the pressure inside the vacuum vessel is 350 Pa. This effect is equivalent to a 60% reduction in the surface force in the atmosphere.

Keywords: surface force; van der Waals force; electrostatic force; liquid bridge force; microstructure; measurement; optical fiber probe; laser diode; coordinate measuring machine (CMM)

1. Introduction

Recent years have witnessed an increased demand for a method for precise measurement of the microstructures of mechanical microparts, microelectromechanical systems, micromolds, optical devices, microholes, *etc.* However, precise measurement of the shape of a microstructure with a large length-to-diameter (L/D) ratio is rather difficult because of the difficulty in probe fabrication and sensing methods where the measuring force is very small. Previous works have reported microstructure measurement techniques that employ a variety of probes such as optical probes, vibroscanning probes, vibrating probes, tunneling effect probes, opto-tactile probes, fiber deflection probes, optical trapping probes, and diaphragm probes [1–9].

In a previous study, we developed a system for the measurement of three-dimensional (3D) microstructures using an optical fiber probe that functions as a kind of displacement measuring probe with a small contact force and wide measurement range [10]. In this system, the shaft of the stylus does not need to be rigid for the detection of the measuring force, because the deflection of the stylus is measured by a non-contact method. In general, when the particle size is less than several tens of micrometers, the effects of surface force generated from the van der Waals force, electrostatic force, and liquid bridge force are strengthened and this surface force becomes greater than the force of gravity [11]. We used a fiber stylus with a 5-μm-diameter sphere on its tip, and as a result, we found

that the measurement surface draws the stylus tip closer when the tip approaches it and the distance between the stylus tip and the measured surface is less than the regular displacement. When the stylus tip comes into contact with the measured surface, it adheres to the surface and cannot be separated from it. When the measured surface is scanned point by point in the touch-trigger mode (Figure 1a), the measurement time increases because the stylus tip is required to be separated from the measured surface to overcome the surface force. When the measured surface is scanned continuously in the scanning mode (Figure 1b), the measurement accuracy reduces because of the bending of the stylus shaft due to the adhesion. The observed adhesion, which is influenced by environmental factors (e.g., humidity) and the roughness of the measurement surface, is not reproducible. Therefore, in another previous work, we developed a measurement system for 3D microstructures that uses a vibrating fiber probe (Figure 1c) to prevent adhesion of the stylus tip to the surface being measured [12]. In this system, the stylus tip is set to vibrate in a circular motion, where it traces a circle of diameter 0.4 μm in the X-Y plane. However, the stylus tip actually traces an elliptical path. The difference between the profile of the perfect circle and that of the actual elliptical path of the stylus tip leads to measurement error. Moreover, the surface roughness cannot be measured in the scanning mode when using the vibrating fiber probe.

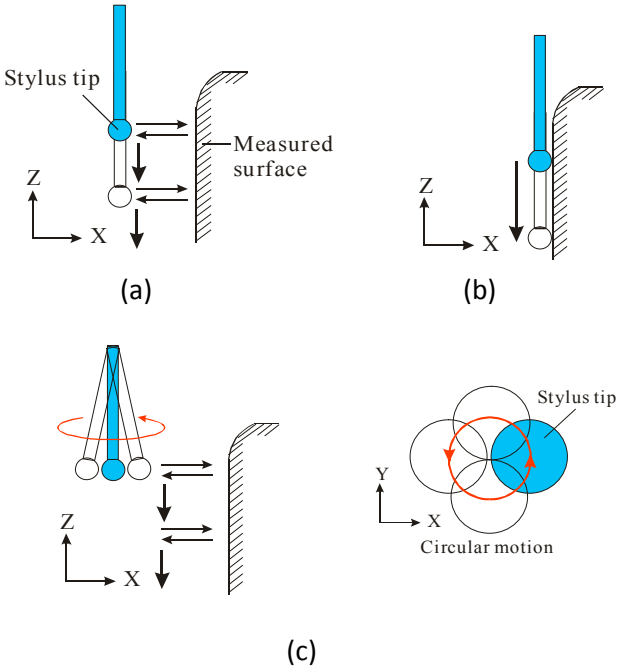

Figure 1. Various types of probes. (**a**) Touch-trigger probe; (**b**) scanning probe; and (**c**) vibrating probe (touch-trigger mode).

In the present study, the stylus characteristics are examined. Then, the effects of the surface force on the adhesion are analyzed. The results confirm that the primary cause of adhesion is the liquid bridge force. Therefore, the measurement system, placed in a vacuum vessel, is constructed suitably to prevent the adhesion caused by the surface force between the stylus tip and the measured surface. The effects of pressure inside the vacuum vessel on the surface force are evaluated experimentally. The surface force is calculated by assuming that the optical fiber probe is equal to the cantilever of the fixed support. In other words, the surface force is calculated by the deflection of the stylus shaft. There are many techniques for measuring surface forces, such as those involving the surface forces apparatus (SFA), atomic force microscopy (AFM), micro cantilever (MC), optical trapping (OT), *etc.* [13–15]. The measuring method that uses the optical fiber probe is, in principle, similar to the SFA

and AFM. As a result, the surface force is found to be 0.13 μN when the pressure inside the vacuum vessel is 350 Pa. This effect is equivalent to a 60% reduction in the surface force in the atmosphere.

2. Measurement Principle

Figure 2 shows a diagram of the developed optical measurement system. The stylus consists of a 2.5-μm-diameter optical fiber to which a 5-μm-diameter glass stylus tip is attached. The total length of the stylus is 0.38 mm. The probing system consists of the fiber stylus, two laser diodes with a 650 nm wavelength (LDX and LDY in the *X*- and *Y*-directions, respectively), and two dual-element photodiodes (PX and PY in the *X*- and *Y*-directions, respectively). The stylus shaft is fixed to a tube-type piezo driver element in order to perform attitude adjustment of the stylus shaft; the stylus shaft is installed between the laser diodes and the dual-element photodiodes, which are oriented orthogonally. The laser diodes are mounted above the stylus tip, and the focused laser beams irradiate along the *X*- and *Y*-directions onto the stylus shaft. The two dual-element photodiodes are located opposite the laser diodes beyond the stylus. The laser beams that pass through the stylus shaft are received by these dual-element photodiodes. The beam intensities detected by the photodiodes are converted into voltages; hereafter, these intensities are denoted as I_{PX1}, I_{PX2}, I_{PY1}, and I_{PY2} (V). The output signal I_X in the *X*-direction obtained using I_{PY1} and I_{PY2} and the output signal I_Y in the *Y*-direction obtained using I_{PX1} and I_{PX2} are defined as given in Equations (1) and (2), respectively. A charge-coupled device is employed to monitor the positions of the stylus and test piece during the setting up of the equipment and the measurement.

$$I_X = I_{PY1} - I_{PY2} \quad (1)$$

$$I_Y = I_{PX1} - I_{PX2} \quad (2)$$

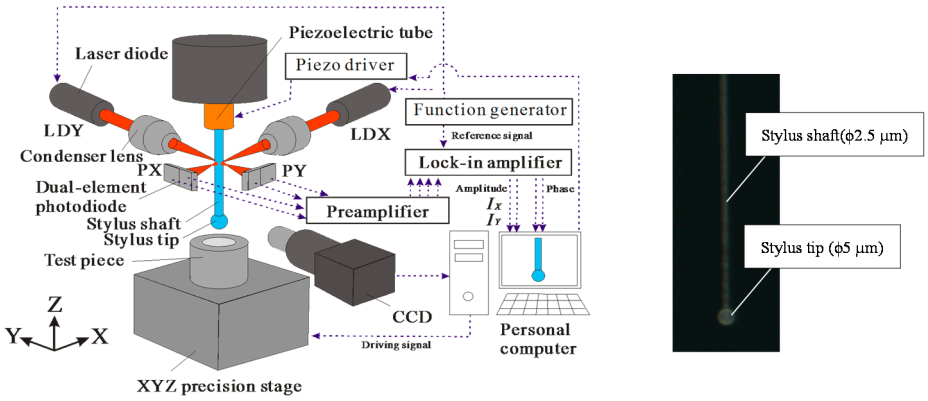

Figure 2. Measurement system using optical fiber probe.

To illustrate the measurement principle of the optical fiber probe, Figure 3 shows a cross-sectional diagram of the *X*-*Y* plane of the optical system shown in Figure 2. Before the stylus tip comes into contact with the measured surface, the light intensities measured by each element of the dual-element photodiode are equal (*i.e.*, $I_{PX1} = I_{PX2}$ and $I_{PY1} = I_{PY2}$), as shown in Figure 3a. When the stylus tip comes into contact with the measured surface in the *X*-direction, the laser-irradiated part of the stylus shaft is displaced, and the light intensities measured by each element of the dual-element photodiode are no longer equal to each other (*i.e.*, $I_{PX1} = I_{PX2}$ and $I_{PY1} > I_{PY2}$), as shown in Figure 3b. When the stylus shaft is displaced in the +*X*-direction, the angle of refraction of the laser beam passing through the stylus shaft in the *Y*-direction changes owing to a shift in the part of the stylus shaft being irradiated. Additionally, when the stylus tip comes into contact with the measured surface in the *Y*-direction, the light intensities measured by each element of the dual-element photodiode are no longer equal to each other (*i.e.*, $I_{PX1} < I_{PX2}$ and $I_{PY1} = I_{PY2}$), as shown in Figure 3c. As a result, the contact direction and

the magnitude of displacement of the stylus tip can be obtained from the output signals I_X and I_Y. When the stylus tip comes into contact with the measured surface in the *Z*-direction, the stylus shaft is buckled and deflected. This deflection is also measured using the above-mentioned method.

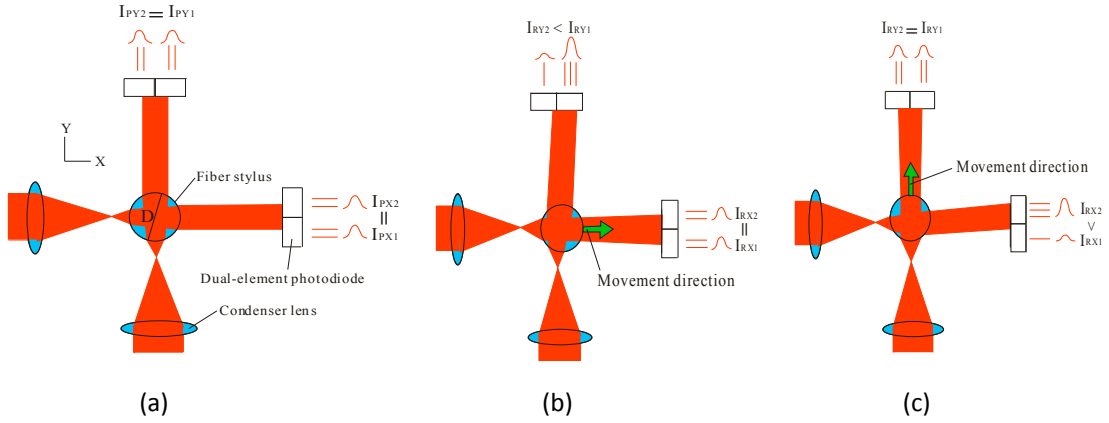

Figure 3. Principle of measurement. (**a**) initial stage; (**b**) displacement in *X*-direction; and (**c**) displacement in *Y*-direction.

Because the proposed probe measures the deflection amplitude of the stylus shaft by using a laser-based non-contact method, the stylus shaft does not need to be rigid; this principle also applies to a stylus with a much smaller diameter. This measurement system measures the deflection of the stylus shaft; however, it does not directly measure the displacement of the stylus tip. The noise present in I_X and I_Y is removed via synchronous detection using a lock-in amplifier. The displacement of the stylus is magnified by using it as a rod lens. The surface of the microstructure is measured by recording the displacement of the stylus shaft as well as the coordinates at which the stylus comes into contact with the measured surface.

3. Stylus Characteristics

Figure 4 shows the changes in outputs I_X and I_Y when the stylus tip is displaced in the $\pm X$-direction. Here, the horizontal axis represents the displacement of the stylus tip and the vertical axis represents the changes in I_X and I_Y. It can be seen that when the stylus tip is displaced in the *X*-direction, barely any change occurs in the output I_Y in the *Y*-direction and the fiber probe can function as a displacement sensor because the rate of change in I_X can approximate a straight line within a ± 3 μm range in the *X*-direction.

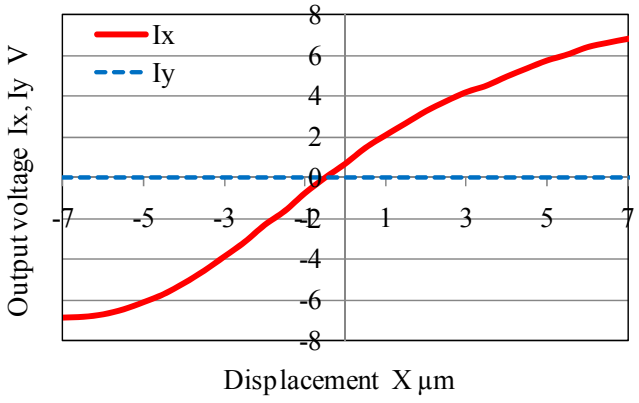

Figure 4. Changes in output voltages I_X and I_Y induced by displacement in $\pm X$-direction.

4. Effects of Surface Force

4.1. Analyses of Liquid Bridge Force, Van der Waals force, and Electrostatic Force

In general, when the particle size is less than several tens of micrometers, the effects of the surface force generated from the van der Waals force, electrostatic force, and liquid bridge force are strengthened and this surface force becomes greater than the force of gravity [11]. Figure 5 shows a schematic diagram of the surface force between the stylus tip and the measurement surface. Because the fiber stylus has a 5-μm-diameter sphere on its tip, the measurement surface draws the stylus tip closer when the stylus tip approaches it, and the distance between the stylus tip and the measured surface is less than the regular displacement. When the stylus tip comes into contact with the measured surface, it adheres to the surface and cannot be separated from it. When the measured surface is scanned point by point in the touch-trigger mode, the measurement time increases because the stylus tip is required to be separated from the measured surface on account of the surface force. When the measured surface is scanned continuously in the scanning mode, measurement accuracy reduced because of the bending of the stylus shaft due to the adhesion. The observed adhesion, which is influenced by environmental factors (e.g., humidity) and the roughness of the measured surface, is not reproducible.

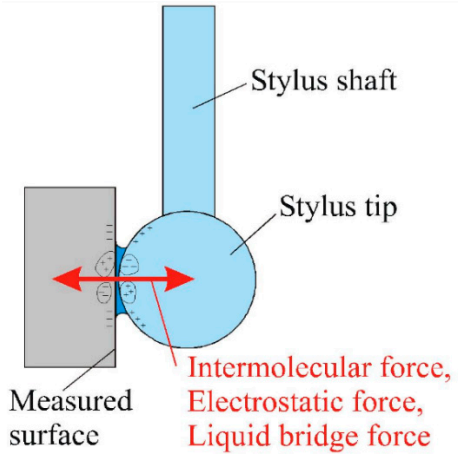

Figure 5. Schematic diagram of surface force between stylus tip and measured surface.

These surface forces are analyzed with the aim of investigating the causes of adhesion. First, we examine the liquid bridge force. This force has a large effect on adhesion in a humid environment; it is generated by the capillary action of condensed water near the contact zone of the stylus tip and measured surface. This force increases with increasing relative humidity. The liquid bridge force F_l experienced in the case of a stylus tip of diameter d and under a relative humidity of $\%RH$ can be calculated using the empirical formula in Equation (3) [11]. This is the empirical formula of the liquid bridge force between a particle and a plate with a hard and clean surface. As indicated by this formula, the liquid bridge force increases with increasing relative humidity.

$$F_l = 0.15d\{0.5 + 0.0045 \times (\%RH)\} \quad (3)$$

Next, we examine the van der Waals force. This force acts between molecules, and it is a general force of interaction that acts between objects at all times. The van der Waals force F_V can be calculated using the Hamaker constant A and the distance z between the stylus tip and the measured surface as given in Equation (4) [11]. The Hamaker constant A is a constant specific to materials, and it is expressed as in Equation (5), where n and Λ are the number of atoms per unit volume and the constant of proportionality of London forces, respectively. When the molecules of the stylus tip and

the measured surface come close to each other by the van der Waals force, intermolecular repulsive force is generated between the molecules of the stylus tip and the measured surface. The molecules are stabilized at the most stable position, which corresponds to the position with the smallest potential energy. At this instant, the separation distance z is about 0.4 nm.

$$F_V = Ad/(12z^2) \quad (4)$$

$$A = n^2 \pi^2 \Lambda \quad (5)$$

Finally, the electrostatic force generated by an interaction between a charged particle and an uncharged surface is examined. When a charged particle comes into contact with an uncharged surface, the generated electrostatic force F_e can be calculated using Equation (6) in the case that the distance between the stylus tip and the measured surface is negligible because it is remarkably small compared with the diameter of the stylus tip [11].

$$F_e = \frac{\pi}{4\varepsilon_0} \cdot \frac{\varepsilon - \varepsilon_0}{\varepsilon + \varepsilon_0} \cdot d^2 \sigma^2 \quad (6)$$

where ε_0, ε, and σ are the dielectric constant of the vacuum, the dielectric constant of the measured surface, and the marginal surface density of the charge of the stylus tip, respectively.

Figure 6 shows the relationship between the stylus tip diameter and the surface forces calculated using Equations (3), (4), and (6). Here, the horizontal axis represents the stylus tip diameter and the vertical axis represents the van der Waals force, electrostatic force, liquid bridge force, and gravity. It can be seen from this figure that when the stylus tip diameter is less than about 1 mm, the effects of surface force generated from the van der Waals force, electrostatic force, and liquid bridge force are strengthened and the surface force becomes greater than the force of gravity.

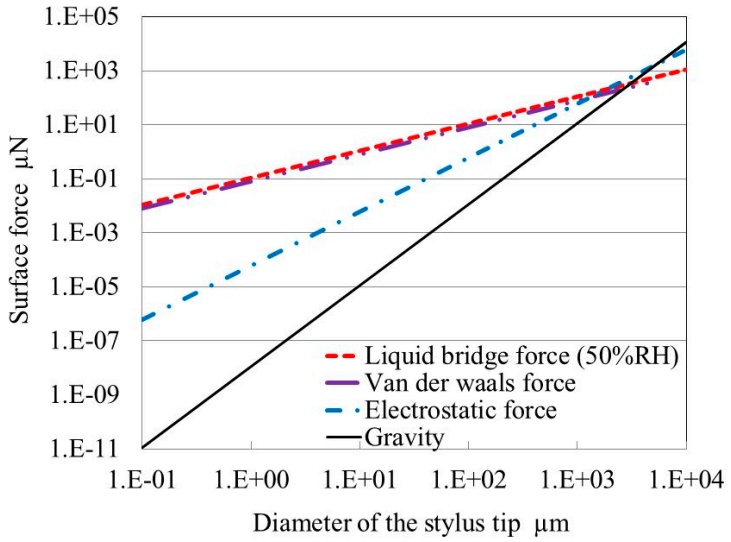

Figure 6. Relationship between stylus tip diameter and surface forces: A (SiO_2) = 1.5 × 10^{-20} J, z = 0.4 nm, ε_0 = 8.85 × 10^{-12} F· m^{-1}, $\varepsilon = \infty$, σ = 26.5 μC· m^{-2}.

This confirms that the primary cause of adhesion is the liquid bridge force. The van der Waals force and liquid bridge force are approximately equal. However, the electrostatic force is much smaller than the van der Waals force and liquid bridge force. When the surface forces are calculated using Equations (3), (4), and (6) for a stylus tip 5 μm in diameter, the liquid bridge force (50% *RH*), van der Waals force, and electrostatic force are 0.54 μN, 0.36 μN, and 0.0016 μN, respectively. In this case, the sum of the surface forces is approximately 0.9 μN. Figure 7 shows the relationship between the relative

humidity and the sum of surface forces ($F_l + F_v + F_e$) calculated using Equations (3), (4), and (6). It can be seen from this figure that the liquid bridge force increases with increasing relative humidity.

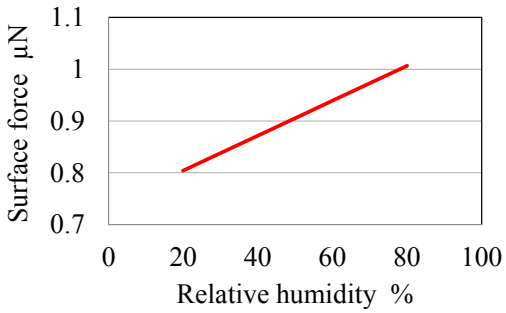

Figure 7. Relationship between relative humidity and surface force (stylus tip diameter: 5 μm).

4.2. Effect of Relative Humidity on the Liquid Bridge Force

As stated in the discussion above, the primary cause of adhesion is the liquid bridge force, which increases with increasing relative humidity. When the measured surface is scanned point by point in the touch-trigger mode, the measurement time increases because the stylus tip is required to be separated from the measured surface on account of the surface force. When the measured surface is scanned continuously in the scanning mode, the measurement accuracy reduces owing to the bending of the stylus shaft due to the adhesion. Therefore, in our previous work, a vibration mechanism was introduced to prevent the adhesion of the stylus tip to the measurement surface caused by the surface force [12]. By this mechanism, the stylus tip is set to vibrate in a circular motion, where it traces a circle of diameter 0.4 μm in the *X*-*Y* plane. However, the stylus shaft actually traces an elliptical path. The difference between the profile of the perfect circle and that of the actual elliptical path of the stylus tip leads to measurement errors. Moreover, the surface roughness cannot be measured in the scanning mode when using the vibrating fiber probe.

Therefore, the measurement system, placed in a vacuum vessel, is constructed suitably to prevent adhesion of the stylus tip to the measured surface caused by the surface force. Figure 8 shows a photograph of the measurement system in the vacuum vessel. The effects of pressure inside the vacuum vessel on the surface force are evaluated experimentally. In the experiment, the relative humidity is 61% and the temperature is 25.1 °C.

First, the measurement method of the surface force is explained as follows. There are many techniques for measuring surface forces, such as those involving the surface forces apparatus (SFA), atomic force microscopy (AFM), micro cantilever (MC), optical trapping (OT), *etc.* [13–15]. The SFA can directly measure the force between two surfaces in controlled vapors or immersed in liquids. The force sensitivity of the SFA is about 10 nN. The SFA contains two curved molecularly smooth surfaces of mica between which the interaction forces are measured using a variety of force-measuring springs. AFM is, in principle, similar to the SFA except that forces are measured not between two macroscopic surfaces but between a fine tip and a surface. The force sensitivity of AFM is 1–10 pN. The measuring method using the optical fiber probe is, in principle, similar to the SFA and AFM. As shown in Figure 9, after the stylus tip comes into contact with the measured surface, the stylus tip is displaced in the backward direction by using the piezoelectric stage, due to which it separates from the measured surface. Because the stylus tip is displaced while maintaining its contact with the measured surface, the stylus shaft is deflected and the force required to separate the stylus tip from the measured surface is generated by the deflection of the stylus shaft. With an increase in the displacement of the stylus tip, this required force also increases. Therefore, the stylus tip can be separated from the measured surface when the displacement D of the stylus tip exceeds a certain value.

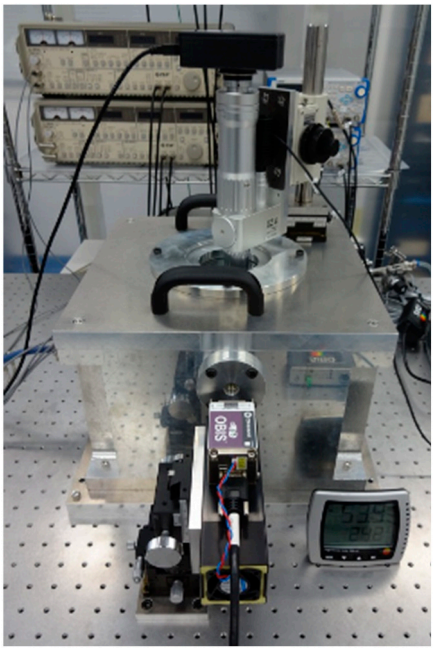

Figure 8. Photograph of measurement system in vacuum vessel.

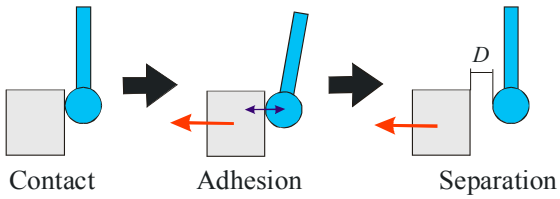

Figure 9. Experimental apparatus for measurement of surface force.

The load acting on the stylus tip, *i.e.*, the surface force, is calculated by assuming that the optical fiber probe, 2.5 μm in diameter and 0.38 mm in length, is equal to the cantilever of the fixed support. In other words, the surface force is calculated by the deflection of the stylus shaft. The surface force F is calculated using Equation (7).

$$F = \frac{3EI}{L^3} \cdot D \tag{7}$$

where E, I, and L are the Young's modulus, the geometrical moment of inertia, and the length of the stylus shaft, respectively. Figure 10 shows the load acting on the stylus tip under the assumption that the stylus shaft (Young's modulus E = 72 GPa) is equivalent to the cantilever of the fixed support. In this figure, the horizontal axis represents displacement of the stylus tip, and the vertical axis represents the load acting on the stylus tip. For example, when the displacement D required to separate the stylus tip from the measured surface is about 20 μm, the load acting on the stylus tip is about 0.15 μN immediately before the stylus tip is separated from the measured surface as shown in Figure 10. Therefore, this value of 0.15 μN is regarded as the surface force. In this experiment, the spring constant of the stylus shaft is not calibrated. However, to accurately measure the surface force, it is necessary to calibrate it [16–19].

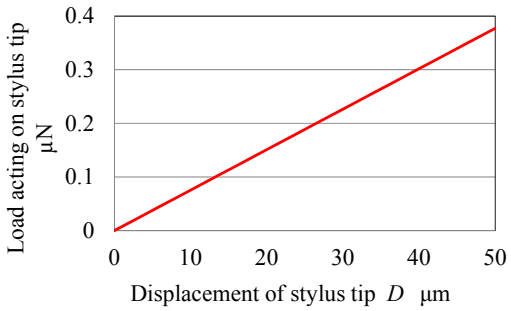

Figure 10. Load acting on the stylus tip (stem length: 0.38 mm, stem diameter: 2.5 μm, and ball diameter: 5 μm).

Figure 11 shows the relationship between the pressure inside the vacuum vessel and the relative humidity. Further, Figure 12 shows the relationship between the pressure inside the vacuum vessel and the surface forces. Finally, Figure 13 shows the relationship between the relative humidity and the surface force. From Figure 13, it is confirmed that surface force decreases with decreasing relative humidity. It is found that the surface force is 0.13 μN when pressure inside the vacuum vessel and relative humidity are 350 Pa and 7% *RH*, respectively. This effect is equivalent to a 60% reduction in the surface force in the atmosphere. However, a large residual surface force still acts between the stylus tip and the measured surface. This is because the amount of van der Waals force is almost the same as that of the liquid bridge force. Therefore, the surface force is thought to reduce by slightly a little more than 60%. When the stylus tip diameter is 5 μm as shown in Figure 6, the theoretical van der Waals force in a vacuum environment is about 0.36 μN. However, according to the obtained experimental results, the van der Waals force in a vacuum environment is about 0.13 μN. Thus, the theoretical and experimental results are different. Because the amount of van der Waals force is affected by the surface roughness of the stylus tip and that of the measurement surface [11], the surface roughness of the stylus tip and that of the measurement surface are, in turn, thought to be affected by the amount of van der Waals force.

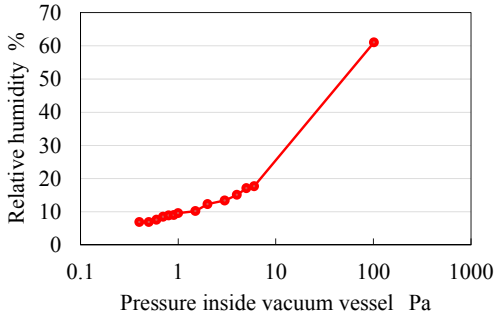

Figure 11. Relationship between pressure inside vacuum vessel and relative humidity.

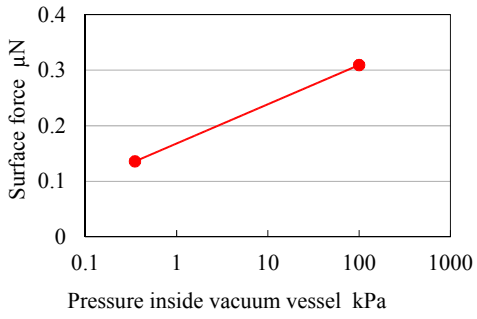

Figure 12. Relationship between pressure inside vacuum vessel and surface forces.

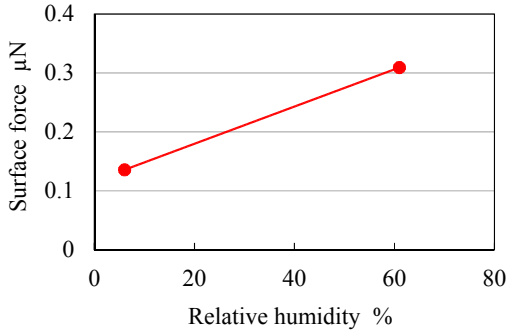

Figure 13. Relationship between relative humidity and surface forces.

4.3. Alternative Reduction Method for Surface Force

According to the above-mentioned experimental results, it is possible to reduce the liquid bridge force considerably by using a vacuum vessel. However, in scenarios where the use of a vacuum vessel is difficult, the stylus tip coated with a water-repellent coating has the potential to reduce the liquid bridge force. In order to reduce the van der Waals force, a stylus tip made of a material with a small Hamarker constant may be used. For example, the Hamaker constants of SiO_2, Fe, Si, Cu, and Au are 8.55, 21.2, 25.6, 28.4, and 45.5 $\times$ 10^{-20} J, respectively. However, in practice, the use of a material with a small low Hamarker constant can be difficult. In such cases, a stylus tip coated with a material with a small Hamarker constant may be used. The effect of the material of the stylus tip can be made negligible by using a coating that is several nanometers thick. The influence of the electrostatic force on the surface force is small; however, it is believed that various methods of removal of electricity or antistatic agents could be useful in reducing the electrostatic force.

5. Conclusions

In this study, the stylus characteristics are examined, and then, surface forces are analyzed in order to investigate the causes of adhesion, which reduces the measurement accuracy. The analysis results of surface forces reveal the liquid bridge force to be the primary cause of adhesion. Therefore, the measurement system placed in the vacuum vessel is constructed suitably to prevent adhesion of the stylus tip to the measured surface because of the surface forces, mainly by reducing the liquid bridge force. As a result, it is found that the surface force is 0.13 μN when the pressure inside the vacuum vessel is 350 Pa. This effect is equivalent to a 60% reduction in the surface force in the atmosphere.

Acknowledgments: This study was partly supported by a research grant from the Mitutoyo Association for Science and Technology and by JSPS KAKENHI Grant Number 26420392.

Author Contributions: Hiroshi Murakami conceived and wrote the paper; Akio Katsuki and Takao Sajima manufactured the vacuum vessel and analyzed the data; Hiroshi Murakami and Mitsuyoshi Fukuda performed the experiments and analyzed the surface forces.

Conflicts of Interest: The authors declare no conflict of interest.

References

1. Masuzawa, T.; Hamasaki, Y.; Fujino, M. Vibroscanning method for nondestructive measurement of small holes. *CIRP Ann.* **1993**, *42*, 589–592. [CrossRef]
2. Hidaka, K.; Saito, A.; Koga, S. Study of a micro-roughness probe with ultrasonic sensor. *CIRP Ann.* **2008**, *57*, 489–492. [CrossRef]
3. Bauza, M.B.; Hocken, R.J.; Smith, S.T.; Woody, S.C. Development of a virtual probe tip with an application to high aspect ratio microscale features. *Rev. Sci. Instrum.* **2005**, *76*. [CrossRef]
4. Claverley, J.D.; Leach, R.K. A vibrating micro-scale CMM probe for measuring high aspect ratio structures. *Microsyst. Technol.* **2010**, *16*, 1507–1512. [CrossRef]

5. Shiramatsu, T.; Kitano, K.; Kawata, M.; Mitsui, K. Development of a measuring method for shape and dimension of micro-components. Modification to the original measuring system, calibration of the probes and the results of dimensional measurements. *JSME Int. J. Ser. C Mech. Syst.* **2002**, *68*, 267–274. [CrossRef]
6. Schwenke, H.; Wäldele, F.; Weiskrich, C.; Kunzmann, H. Opto-Tactile sensor for 2D and 3D measurement of small structures on coordinate measuring machines. *CIRP Ann.* **2001**, *50*, 361–364. [CrossRef]
7. Muralikrishnan, B.; Stone, J.A.; Stoup, J.R. Fiber deflection probe for small hole metrology. *Precis. Eng.* **2006**, *30*, 154–164. [CrossRef]
8. Michihata, M.; Takaya, Y.; Hayashi, T. Development of the nano-probe system based on the laser-trapping technique. *CIRP Ann.* **2008**, *57*, 493–496. [CrossRef]
9. Liebrich, T.; Knapp, W. New concept of a 3D-probing system for micro-components. *CIRP Ann.* **2010**, *59*, 513–516. [CrossRef]
10. Murakami, H.; Katsuki, A.; Onikura, H.; Sajima, T.; Kawagoishi, N.; Kondo, E. Development of a system for measuring micro hole accuracy using an optical fiber probe. *J. Adv. Mech. Des. Syst. Manuf.* **2010**, *5*, 995–1004. [CrossRef]
11. Okuyama, K.; Masuda, H.; Morooka, S. *Biryushi Kogaku*; Ohmsha: Tokyo, Japan, 1992.
12. Murakami, H.; Katsuki, A.; Sajima, T.; Suematsu, T. Study of a vibrating fiber probing system for 3-D micro-structures: Performance improvement. *Meas. Sci. Technol.* **2014**, *25*. [CrossRef]
13. Israelachvili, J.N. *Intermolecular and Surface Forces: Revised Third Edition*; Academic Press: Waltham, MA, USA, 2011; pp. 227–247.
14. Lee, M.; Kim, B.; Kim, J.; Jhe, W. Noncontact friction via capillary shear interaction at nanoscale. *Nat. Commun.* **2015**, *6*. [CrossRef] [PubMed]
15. Yongho, S.; Wonho, J. Atomic force microscopy and spectroscopy. *Rep. Prog. Phys.* **2008**, *71*. [CrossRef]
16. Guebum, H.; Ahn, H.S. Calibration of effective spring constants of colloidal probes using reference cantilever method. *Coll. Surf. A Physicochem. Eng. Asp.* **2015**, *489*, 86–94.
17. Song, Y.P.; Wu, S.; Xu, L.Y.; Zhang, J.M.; Dorantes-Gonzalez, D.J.; Fu, X.; Hu, X.D. Calibration of the effective spring constant of ultra-short cantilevers for a high-speed atomic force microscope. *Meas. Sci. Technol.* **2015**, *26*. [CrossRef]
18. Slattery, A.D.; Blanch, A.J.; Ejov, V.; Quinton, J.S.; Gibson, C.T. Spring constant calibration techniques for next-generation fast-scanning atomic force microscope cantilevers. *Nanotechnology* **2014**, *25*. [CrossRef] [PubMed]
19. Slattery, A.D.; Blanch, A.J.; Quinton, J.S.; Gibson, C.T. Calibration of atomic force microscope cantilevers using standard and inverted static methods assisted by FIB-milled spatial markers. *Nanotechnology* **2013**, *24*. [CrossRef] [PubMed]